Journal of Structural Geology, Vol. 4, No. 3, pp. 271 to 289, 1982
Printed in Great Britain

0191-8141/82/030271-19 $03.00/0

Interrelations of mesoscopic structures and strain across a small regional fold, Virginia Appalachians

ROBERT I. SIMON

Chevron U.S.A., P.O. Box 6056, New Orleans, LA 70174, U.S.A.

and

DAVID R. GRAY

Department of Geological Sciences, Virginia Polytechnic Institute & State University, Blacksburg, VA 24061, U.S.A.

(*Received* 23 *June* 1981; *accepted in revised form* 26 *March* 1982)

Abstract—Small regional folds, such as the Clover Hollow anticline of the Narrows thrust-sheet in southwest Virginia, U.S.A., are considered to be large buckle folds expressing lateral shortening above a subsurface décollement. Cleavage, mesoscopic and regional folds, and contraction faults have developed in these rocks under anchimetamorphic conditions, in a single, protracted deformation during thrust-sheet emplacement. The contraction faults dominate the structure at all scales. Three fault associations (isolated contraction faults, contraction faults in series and complex fault zones with intense folding) determine the pattern and intensity of local structures. Regional displacement transfer of strain along and across faults has produced local variations in structural style. Duplex-like systems of second-order faults terminate laterally into zones of intense folding and third-order faulting. Fold tightness, cleavage intensity, strain magnitude and total longitudinal strain (ε_T) are maximum in these regions. Contraction faults in this thrust-sheet have propagated along zones of high strain rate associated with mesoscopic folding and intense cleavage. Regional hinge migration, and greater structural complexity along the southeast limb of the Clover Hollow anticline, are considered to be due to emplacement of the adjacent thrust-sheet.

INTRODUCTION

KNOWLEDGE of strain distribution and the strain history of regional folds (e.g. Cloos 1947, Mitra 1978, Tan 1976, Milnes 1971) should enable greater understanding of fold kinematics (Ramsay 1967, Hobbs 1971, Milnes 1971). Geometric relations between mesoscopic structures (cleavage, minor folds and faults) and regional folds is also necessary input to determine the deformation history and the relative sequence of accumulated strains. At present, data on folds within the thrust-dominated southern Appalachians is limited. Directions, types and magnitudes of total strain within regional folds are largely unknown.

This paper documents geometrical relations of structural elements, deformation patterns, and spatial variation in total strain associated with a small regional fold in a folded thrust-sheet of the southern Appalachian foreland zone. The aim is to categorize the structural style and to determine the palaeokinematics of regional structural development by investigation of the succession of minor structures and delineation of the related strains. Strain patterns are used to determine whether regional folds formed above ramps due to steplike upward shearing of detachment thrusts (Rich 1934, Gwinn 1964, Harris & Milici 1977), or due to buckle shortening associated with movement on a subsurface décollement.

GEOLOGIC SETTING

The southern portion of the foreland fold- and thrust-belt of the Appalachian orogen is characterized by arcuate, discrete, discontinuous fault traces which truncate regional anticlines and synclines (Fig. 1). Regional faults are either listric or steplike with multiple décollement levels, and join a master décollement at depth (Fig. 2). Three major thrust slices are recognized in this portion of the Valley and Ridge Province: the Pulaski, Saltville and Narrows thrust-sheets (Fig. 1b). The anticline investigated is the Clover Hollow anticline situated in the Narrows thrust-sheet, which is approximately 16 km in width. Low temperature (180–230°C) deformation for this sheet is inferred from conodont colour alteration (Epstein *et al.* 1976). Regional structures within this sheet include large dome and basin structures with half-wavelengths of 8 km, large elongate regional folds (near the southern-central Appalachian juncture zone) with half-wavelengths of 6.4 km and strike-lengths up to 45 km, and smaller regional folds with half-wavelengths of 6 km and strike-lengths up to 13 km. The small regional folds occur at the northeast and southwest terminations of the large dome structures (Fig. 1b).

The Clover Hollow anticline is a doubly-plunging, slightly asymmetric, small regional-fold. It is located

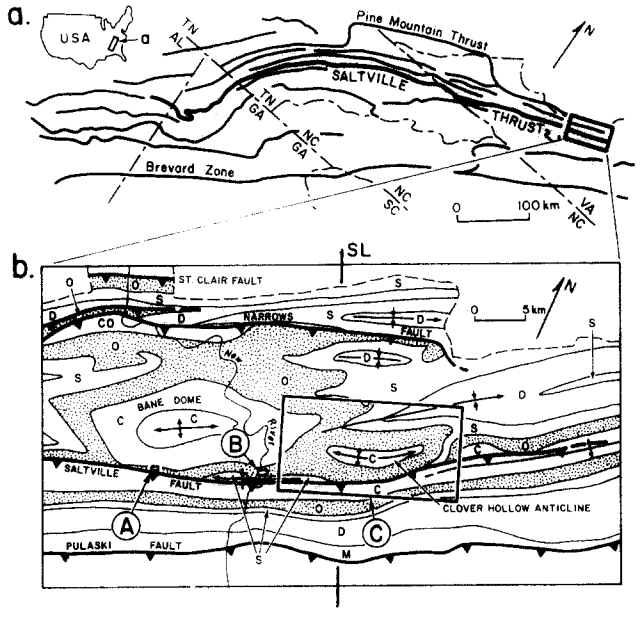

Fig. 1. Location maps. (a) Traces of major regional thrusts in the southern Appalachian foreland zone (TN, Tennessee; AL, Alabama; NC, North Carolina; GA, Georgia; SC, South Carolina and VA, Virginia) (b) Geologic map of the northern portion of the Narrows thrust-sheet and adjacent sheets in southwestern Virginia. C, Cambrian; O, Ordovician (stippled pattern); S, Silurian; D, Devonian and M, Mississippian. A, B and C indicate positions of Figs. 11, 10 and 3, respectively. SL section line for Fig. 2.

adjacent to the Saltville thrust between the Bane Dome to the southwest and much larger folds to the northeast (Fig. 1). The anticline trends approximately N57°E, has a strike-length of 26 km and a quarter-wavelength of 5 km (Fig. 3). Lithologic contrasts in the local stratigraphy (Fig. 4) create a multilayer package with competent and incompetent layers exhibiting different structural style. Exposed lithologies range from Cambrian to Silurian in age. Two structurally-important lithologic groupings are: the Moccasin Formation, a maroon calcareous mudrock subdivided into a basal reddish to white argillaceous limestone, a red calcareous mudrock and sandy mudrock to pure sandstone; and Middle Ordovician Limestones, subdivided into argillaceous limestone, dolomitic limestones and skeletal limestone.

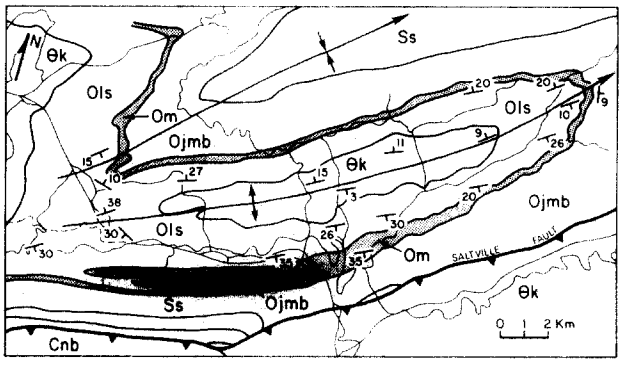

Fig. 3. Geologic map of the Clover Hollow anticline and showing the trace of the Saltville fault. Lithologies include: Cnb, Honaker Dolomite; θk, Knox Dolomite; Ols, Middle Ordovician limestones; Om, Moccasin Formation; Ojmb, Eggleston, Martinsburg, Juniata Formations and Ss, Silurian sandstones. The location of Fig. 3 is shown in Fig. 1 (b).

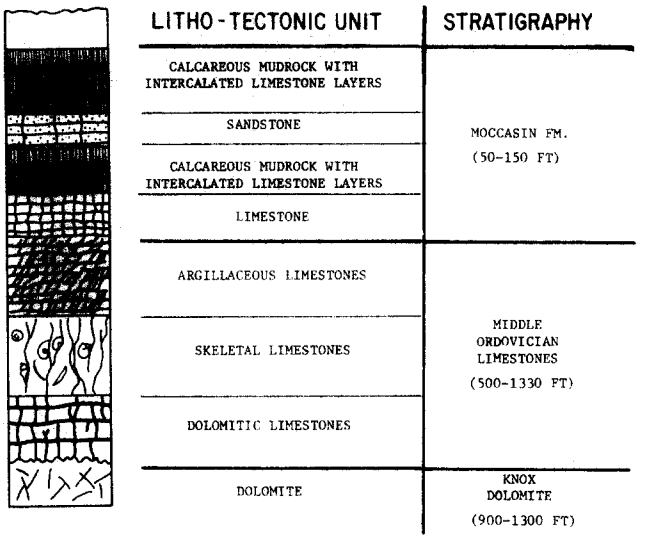

Fig. 4. Local stratigraphy showing litho-tectonic subdivisions and respective cleavage morphologies, is modified from Alvarez *et al.* (1978), Powell (1979) and Geiser & Sansone (1981).

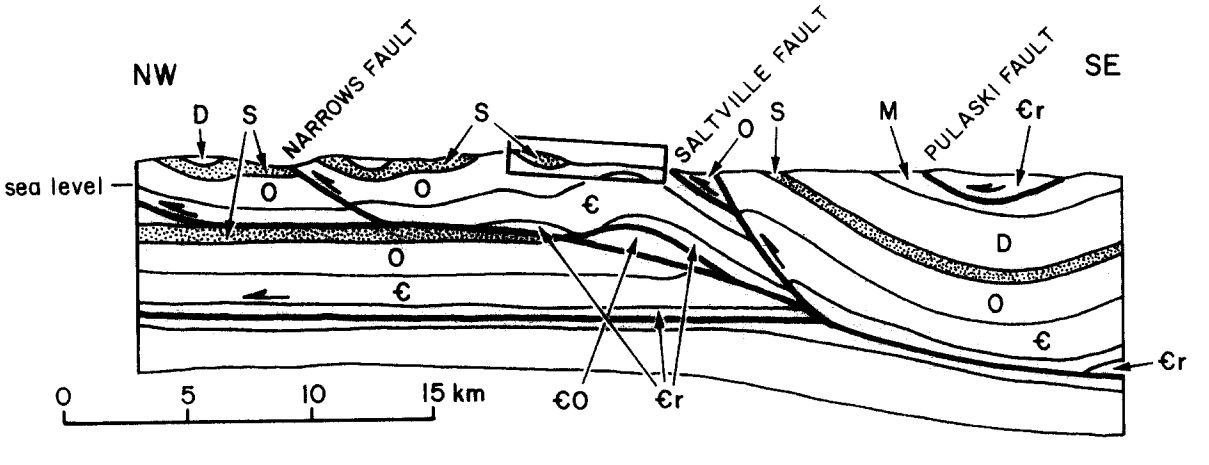

Fig. 2. Interpretative regional cross-section through the Narrows and adjacent thrust-sheets (from Milici 1970, fig. 6). The position of Fig. 17(b) is shown by the rectangle. Key as Fig. 1; ϵ, ϵo and ϵr are Cambrian formation after Milici.

Cambro-Ordovician dolomites (Knox Dolomite) in the core of the anticline are medium- to thick-bedded, cherty-dolomites with some interbedded limestones.

STRUCTURAL ELEMENTS

Important structural elements in the Narrows thrust sheet are mesoscopic folds, faults and cleavage (Fig. 5). They define the structural style within the thrust sheet and reflect the palaeokinematics of regional structural development. Each structural element will be treated separately. Locations of structure sections referred to in the paper are shown in Fig. 6.

Faults

Different orders of contraction-faults (cf. Price 1967) characterize this portion of the Appalachian Valley and Ridge Province. First-order faults are regional thrusts which have displacements of tens of kilometres with strike-lengths of hundreds of kilometres (Fig. 1a). Second-order contraction faults have displacements of tens of metres and strike-lengths up to 2–3 km (Fig. 7a). Third-order contraction faults have displacements less than 10 m, generally 1–3 m, and strike-lengths less than 0.5 km (Figs. 8a & c). Minor small-scale (third-order) extension faults are also present.

Second- and third-order contraction faults dominate the structural pattern on the southeast limb of the Clover Hollow anticline, producing marked tectonic thickening of the Moccasin Formation (Fig. 3) and partial repetition of the stratigraphic succession (Fig. 9a). Third-order faults in mudrock are often parallel to cleavage. They are distinguished by shear veins (Ramsay 1981, fig. 10C); that is slickensides composed of layers of fibrous calcite (up to 1 cm thick), on cleavage surfaces. Many faults modify cleavage. Increased cleavage intensity, reorientation of cleavage and modification of cleavage micro-fabric adjacent to faults reflect this.

Three associations of second-order contraction faults have been recognized.

(1) *Isolated faults in relatively undeformed strata.* Fault strike-lengths are up to 1 km and displacements up to tens of metres. They occur as single, discrete fault surfaces at the base of the Moccasin Formation (Fig. 7a). Middle Ordovician limestones (Fig. 7b, sections A–A′ and C–C′) or basal Moccasin limestones (Fig. 7b, section B–B′) are thrust over basal Moccasin strata. Both cleavage and folds are modified by these faults (Fig. 7a).

(2) *Contraction faults in series.* Subparallel contraction faults define narrow zones (up to 0.5 km wide) where imbricate slices repeat the stratigraphy from the Middle Ordovician limestones to the Martinsburg Formation (Fig. 9a). Strike-lengths are up to 2–3 km. Individual contraction faults are either groups of smaller faults (Fig. 9c, section G–G′) or discrete fault surfaces (Fig. 9c, sections H–H′ and I–I′). The zones terminate laterally into highly folded strata cut by numerous third-order contraction faults (Fig. 8). Both groups of faults truncate folds and cleavage, and have rotation axes of 8°/N74°E.

(3) *Complex fault zone.* Second-order contraction faults are associated with third-order contraction faults and intense folding (Fig. 10 section J–J′). These zones occur in the lower part of the Moccasin Formation. Incipient rampfaults in folded uppermost Middle Ordovician limestones represent the base of the zones (Fig. 10b). Third-order faults have variable displacements terminating upsection as bedding-parallel thrusts (Fig. 10d) or small localized high-angle reverse faults (Fig. 10c). Competent sandstone units exhibit anastomosing splay-networks of faults which cause multiple wedging of layering (Fig. 10d).

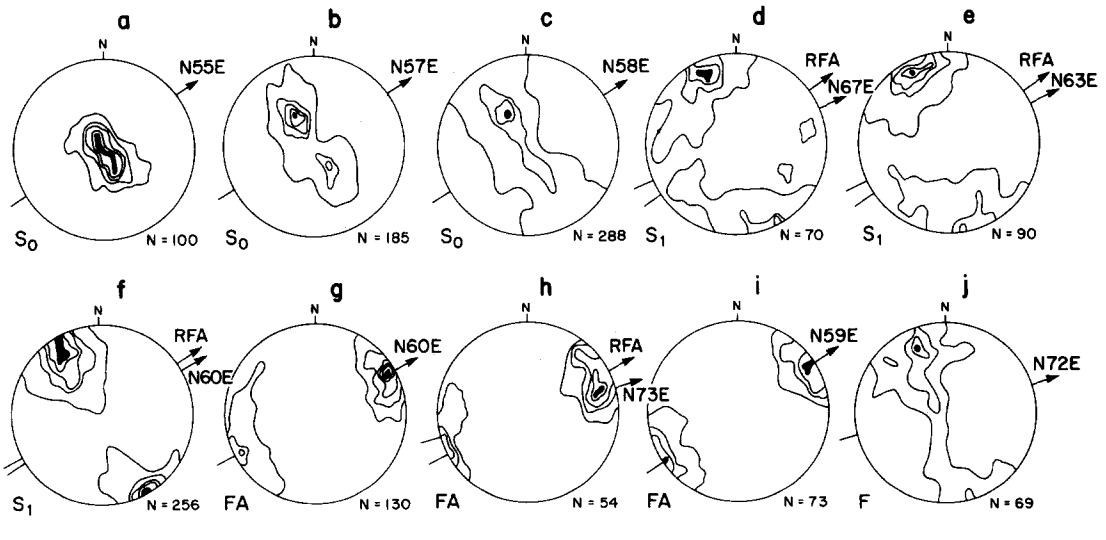

Fig. 5. Structural orientation data for the Clover Hollow anticline, equal-area (Schmidt) projections. RFA is the regional fold axis trend. (a) Knox Dolomite; poles to bedding; confidence interval (C.I.) = 5%. (b) Middle Ordovician limestones; poles to bedding; C.I. = 5%. (c) Moccasin Formation; poles to bedding; C.I. = 4%. (d) Middle Ordovician limestones; poles to cleavage; C.I. = 5%. (e) Basal Moccasin limestone; poles to cleavage; C.I. = 5%. (f) Moccasin mudrock; poles to cleavage; C.I. = 3%. (g) Total mesoscopic fold axes; C.I. = 5%. (h) Group 2 fold axes; location 1, Fig. 6; C.I. = 5%. (i) Group 1 fold axes; location 2, Fig. 6; C.I. = 5%. (j) Third-order faults; poles to fault planes; C.I. = 5%.

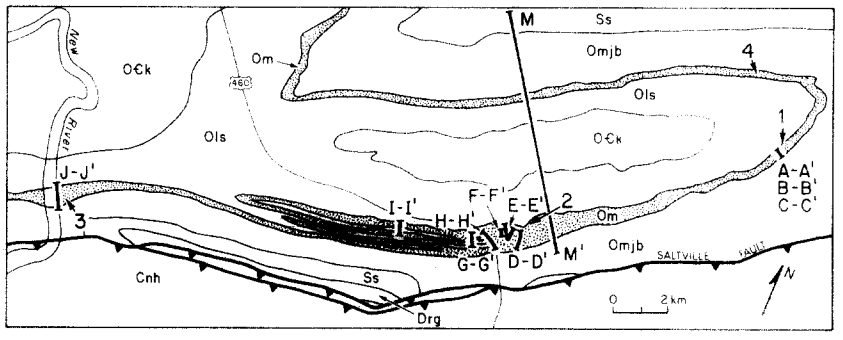

Fig. 6. Location map of structural sections (denoted by letters) and locations where total longitudinal strain (ε_T) was calculated (numbers correspond to those in Table 3). The Moccasin Formation (Om) is stippled. Oεk, Knox dolomite; Ols, Middle Ordovician limestones; Omjb, Eggleston, Martinsburg and Juniata Formations and Ss, Silurian sandstones.

Each association contains a detachment zone at or along the contact between the Moccasin Formation and underlying Middle Ordovician limestones (Figs. 7b, 9a and 10c). This zone, 1–3 m thick, within the basal limestone member of the Moccasin formation, is distinguished by tight, chevron-like, polyclinal folds (Fig. 7b, sections B–B′ and C–C′) structurally disharmonic with the more open, sinusoidal fold forms in both the Moccasin mudrock and Middle Ordovician limestones immediately above and below the detachment surfaces (Fig. 7b, section A–A′). Other characteristic features of these zones are bedding-parallel faults, small low and high angle reverse faults with displacements less than 1 m, and small wedge faults associated with folds (Fig. 10c).

Folds

Two orders of folds are recognized. Large-scale regional structures (first-order) have wavelengths up to 12 km and strike-lengths up to 13 km. Mesoscopic (second-order) folds within these structures, occur in the Middle Ordovician limestone and Moccasin Formation. These are divided into two distinct fold groups based on structural association, geometry and distribution within the Clover Hollow anticline.

Group 1. These comprise both isolated folds in relatively undeformed strata and fold complexes associated with third-order contraction faults (Figs. 8 and 11). Fold style varies with lithology. Broad, open folds with wavelengths of 10–40 m and amplitudes of 3–20 m occur in the thick-bedded Middle Ordovician limestones (Figs. 10 and 11d). These are upright to gently plunging with rounded hinges and interlimb angles of 80–120°. Fold geometry is either class 1B or 1C (Ramsay, 1967). Folds in the Moccasin Formation have wavelengths 4–12 m, amplitudes of 1–3 m and interlimb angles of 40–90°. Hinges are rounded in the thick basal limestone and calcareous mudrock litho-tectonic units, and chevron in thin limestone–mudrock multilayer packages. Geometries vary from class 1B/1C to class 3 in calcareous mudrock.

The majority of these mesoscopic folds are transected

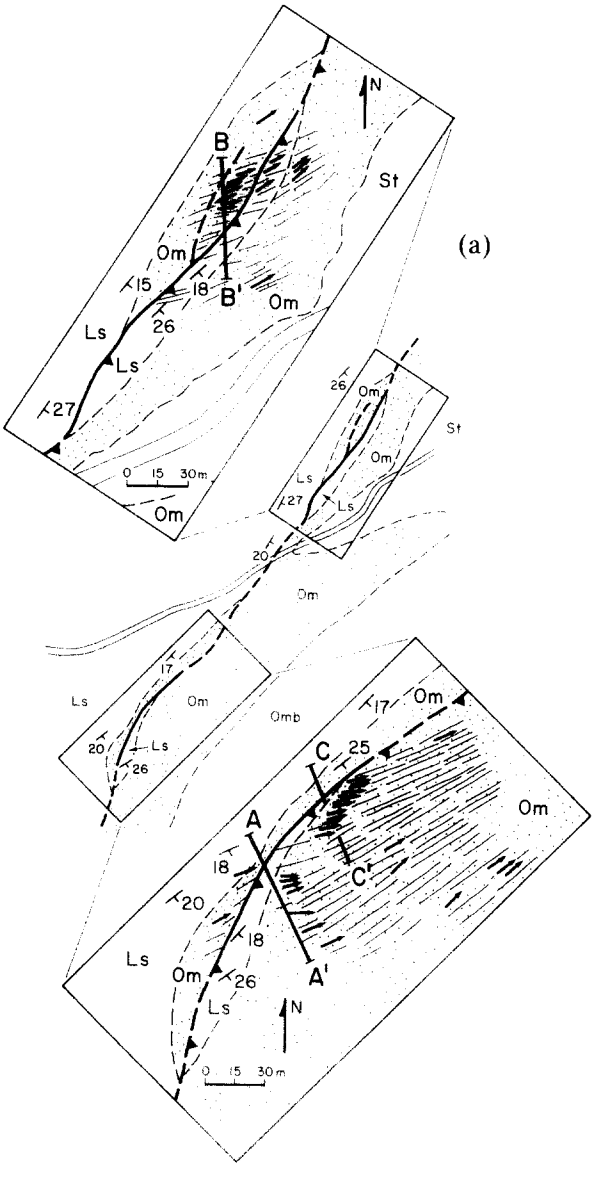

Fig. 7. Geologic maps and structural sections of an isolated second-order contraction fault near the nose of the Clover Hollow anticline (Location 1, Fig. 6). (a) Maps showing structural relations between the fault (heavy trace with teeth), cleavage traces (thin lines) and fold axes (arrows). Ls, Middle Ordovician limestone; Om, Moccasin Formation; Omb, Eggleston and Martinsburg Formations and St, Silurian talus.

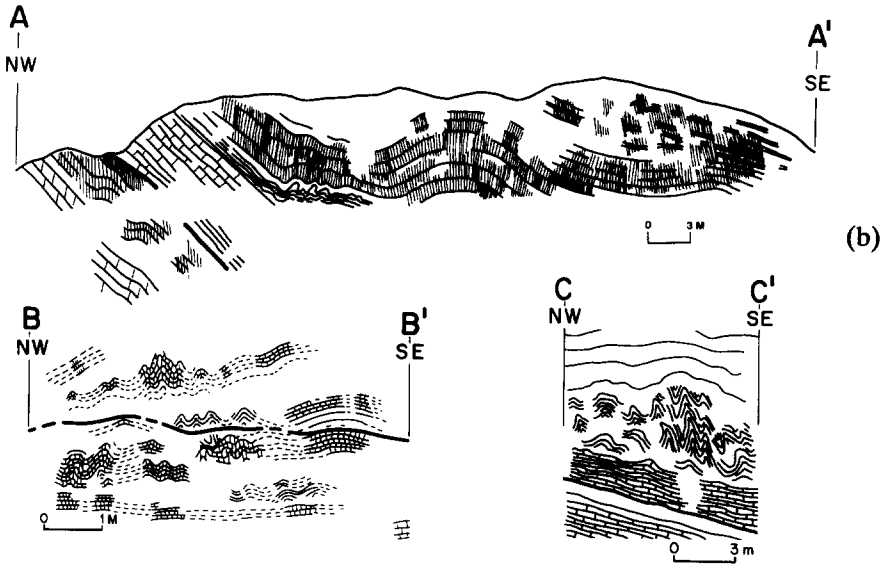

Fig. 7 (b) Structural sections A–A′, B–B′ and C–C′ (see part (a) for location). The fault trace is shown by the heavy line.

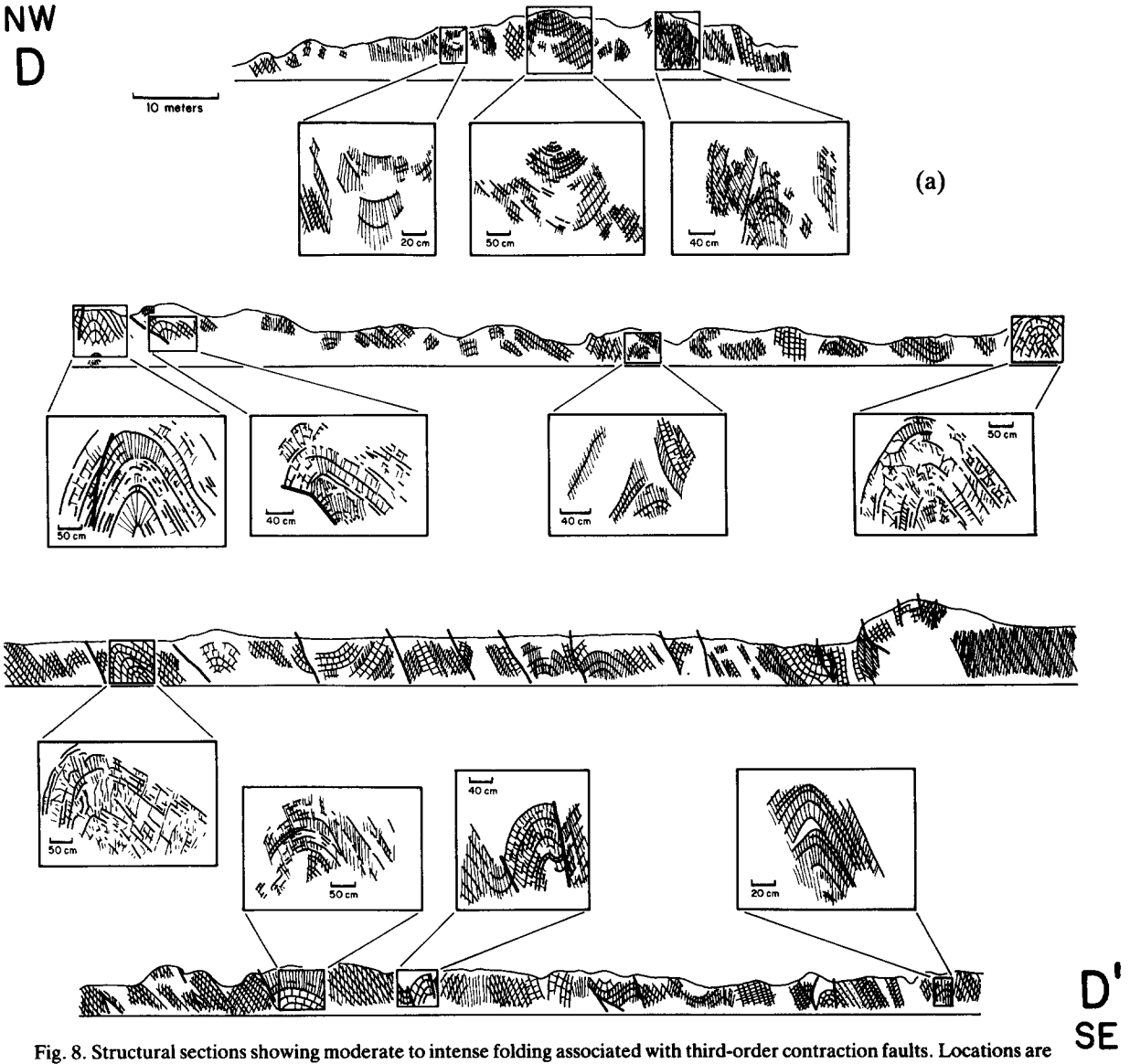

Fig. 8. Structural sections showing moderate to intense folding associated with third-order contraction faults. Locations are shown in Fig. 6. (a) D–D′: road outcrop, county route 601.

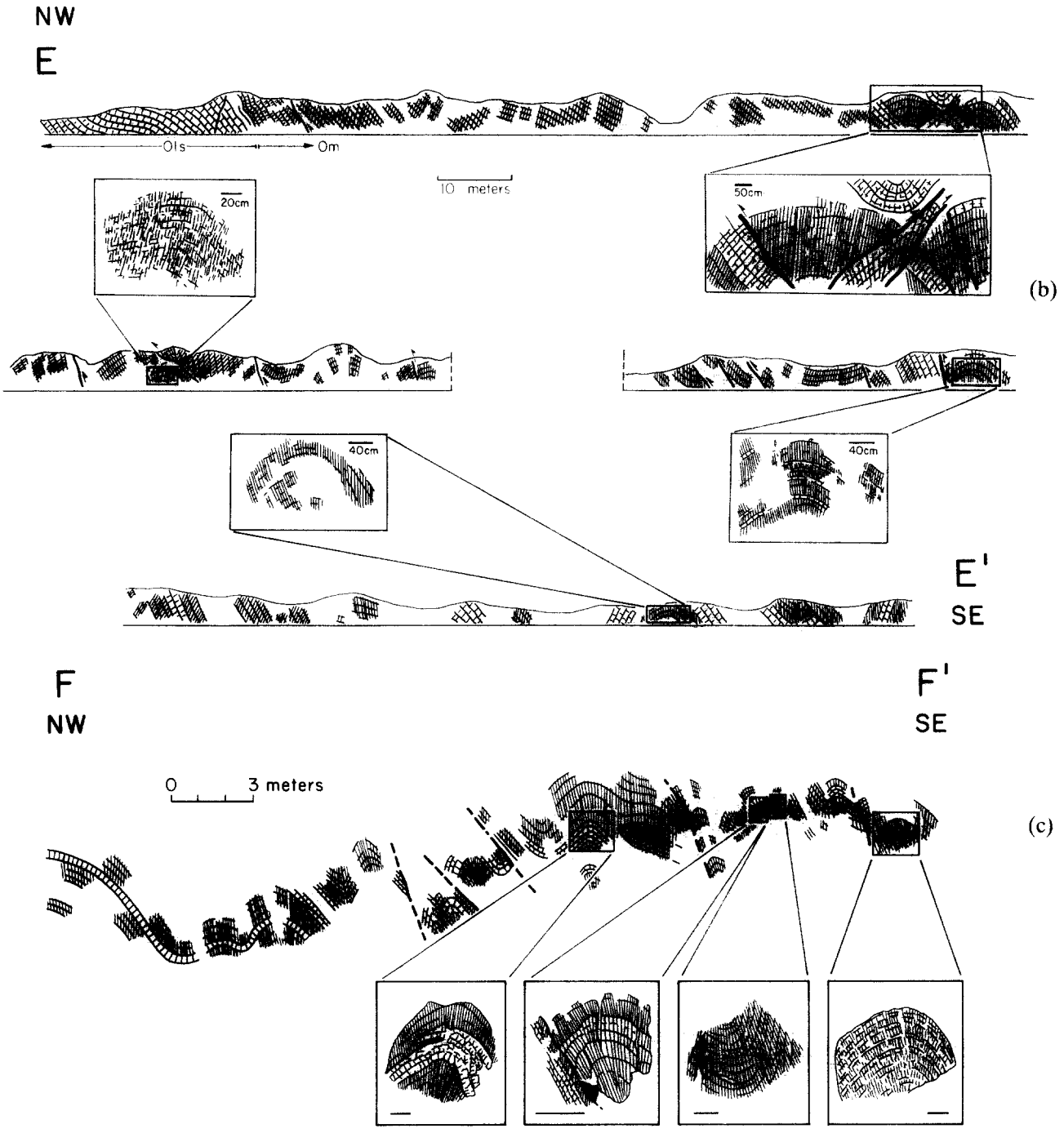

(b) E–E′: road outcrop, county route 604. (c) F–F′: hillside outcrop above Sinking Creek. (Bar scales for folds are 0.4 M).

by cleavage and occur on the southeast limb of the Clover Hollow anticline (see Gray, 1981a). They form a complex sequence of anticlines ramped over anticlines (Figs. 8a & c). Synclinal hinges, commonly faulted out, are only present where thick limestone and sandstone layers occur in their outer arcs (Figs. 8b & c). Few mesoscopic folds occur on the northwest limb of the regional structure. They are isolated broad open folds with interlimb angles ranging from 80 to 150°.

Group 2. These mesoscopic folds are associated with second-order contraction-faults and bedding-parallel detachments (Fig. 7b, section C–C′, and Fig. 11d, section L–L′). They have tight chevron-like polyclinal shapes with multiple axial planes, diverse orientations and extreme thickening of hinges relative to limbs. Geometries are alternating class 1C and 3 forms. Convolute dip-isogon patterns (Ramsay 1967) are common. Wavelengths range from 0.2 to 2 m, amplitudes from 0.5 to 2 m and interlimb angles from 30 to 100°. Layer-slip features and small contraction faults wedge material into fold hinges.

Group 2 folds occur in the uppermost Middle Ordovician limestones and the basal limestone unit of the Moccasin Formation (Fig. 7b, 9b, and 11b). Their attitude and tightness are related to the presence of the contraction faults and detachment surfaces. Tight,

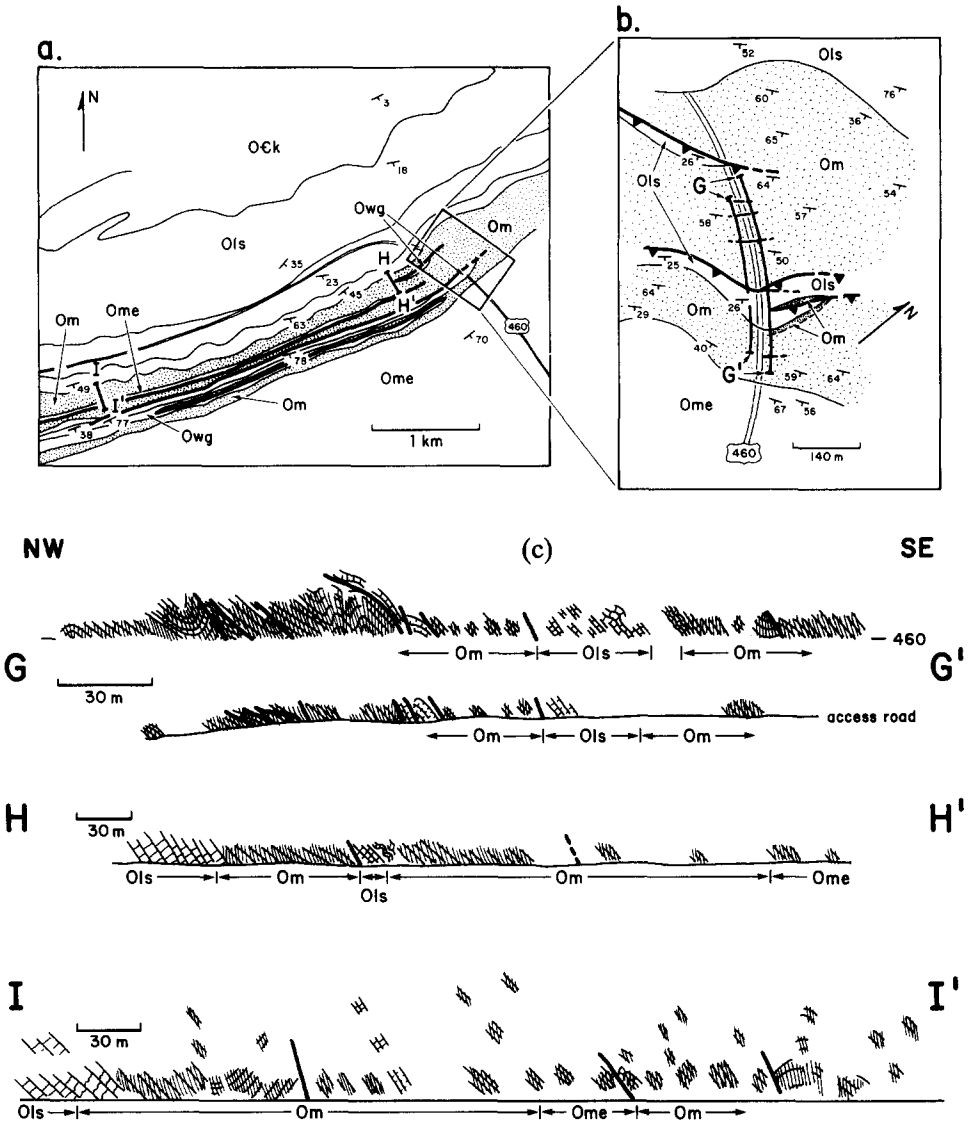

Fig. 9. Contraction faults in series. (a) Geologic map of southeast limb of the Clover Hollow anticline showing a zone of second-order contraction faults, (heavy lines). (b) Map of terminal portions of the faults shown in (a). Third-order faults as well as detachment zones (heavy stipple) are shown within the basal Moccasin Formation. (c) structural sections G–G', H–H' and I–I' (Fig. 6). O€k, Knox Dolomite; Ols, Middle Ordovician limestone inclusive of Owg (Whitten Limestone); Om, Moccasin Formation and Ome, Eggleston and Martinsburg Formations.

polyclinal folds in the overthrust strata die out less than 4 m from fault surfaces (Fig. 7b). Overlying mudrock is gently folded and contains both cleavage and folds of regional orientation. Adjacent to second-order contraction faults, folds diverge up to 20° from regional trends (Fig. 7a). In areas where the stratigraphic contact is structurally conformable, the basal limestone is not folded.

Cleavage

Spaced cleavage occurs within the Middle Ordovician limestones and overlying Moccasin Formation. Cleavage ranges from a close-spaced (40 μm spacing) domainal microfabric (Fig. 12) to a wider-spaced (1–5 cm), spaced disjunctive variety (cf. Powell 1979). The domainal microfabric only occurs in calcareous mudrocks and is transitional with, but locally overprinted by, the spaced disjunctive variety (Gray, 1981b). Cleavage in the limestones has stylolitic form.

The morphology and development of cleavage in the Middle Ordovician limestones and the Moccasin Formation is variable across the Clover Hollow anticline. A degree of cleavage development, weak, moderate and strong, may be defined by cleavage domain thickness and spacing (Table 1). Increasing intensity is categorized by thicker cleavage domains and closer spacing. Gradual variations occur within individual lithological units, whereas sharp contrasts in both cleavage spacing and thickness are found between differing lithologies (Table 2). Regional patterns of cleavage intensity within the Middle Ordovician limestones and Moccasin Formation delineate three strike belts (Fig. 13). These correspond to weak to moderate cleavage intensity along the northwest limb, moderate to strong cleavage intensity near the nose and hinge, and moderate to strong cleavage

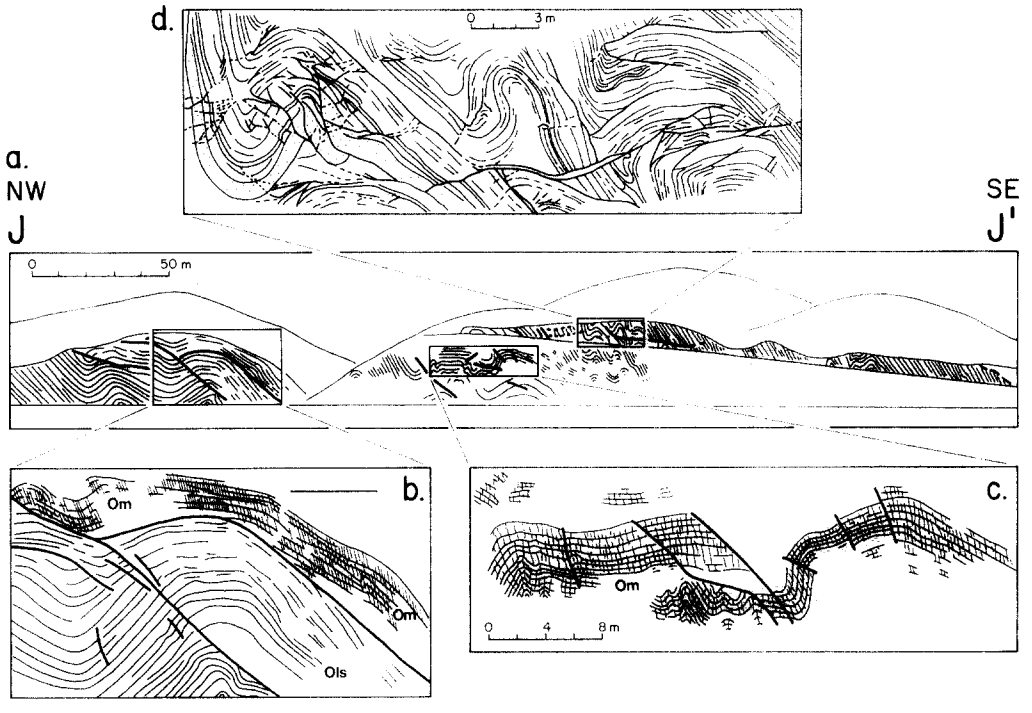

Fig. 10. Complex fault zone. (a) Structural section J–J′ showing second-and third-order contraction faults. (Road, rail and hillside outcrops along the New River near Goodwins Ferry, VA.) Location is shown in Fig. 6. (b) Incipient ramp faults in the folded upper portion of the Middle Ordovician limestones. (c) Detachment zone deformation features in the basal Moccasin limestone. (d) Complex fold, fault, and cleavage relations in the Moccasin and Eggleston Formations along road cut, county route 625. Ols, Middle Ordovician limestone; Om, Moccasin Formation and Ome, Eggleston and Martinsburg Formations.

intensity along the southeast limb (Table 2). Cleavage intensity increases toward regional fold hinges, and is stronger in areas of mesoscopic folds and second-order faults. Maximum cleavage intensity coincides with second- and third-order faults along the southeast limb of the Clover Hollow anticline (Fig. 13). Strong cleavage is localized near the faults, with both hanging and footwall blocks exhibiting variation in cleavage intensity and orientation. Mudrock cleavage microfabrics become more penetrative, characterized by higher dimensional-preferred orientation of clays and elongate calcite grains, adjacent to these contraction-faults (cf. Figs. 12 and 14).

Cleavage orientation also varies across the regional structures (Fig. 15). Stylolitic forms in the limestones on the northwest limb and near the hinge of the Clover Hollow anticline are approximately coplanar to the axial plane trace, while cleavage on the southeast limb is more varied in orientation. Cleavage traces in both mudrock and limestone along this limb are consistently oblique to the regional trend. Deviations are lithology-dependent; competent limestones exhibit higher deviations than calcareous mudrock. Δ transection values, where Δ is the minimum angle between cleavage and the fold axis (Borradaile 1978) have been determined from the regional structural orientation data (Fig. 5): Δ is $-10°$ for the Middle Ordovician limestones, $-8°$ for the basal limestone of the Moccasin Formation and $-2°$ for the calcareous mudrock. This regional transection is also depicted in the cleavage orientation map (Fig. 15). Cleavage also transects mesoscopic folds but there is no consistent pattern of transection (Fig. 16). These relationships are discussed by Gray (1981a).

Local variations in cleavage orientation are associated with second-order contraction faults (Fig. 7a). Cleavage adjacent to faults may deviate up to 50° away from the regional orientation; the traces follow arcuate patterns as cleavage-orientation changes are gradual rather than abrupt.

STRAIN ANALYSIS AND STRAIN STATE

Several competing deformation mechanisms contributed to the bulk deformation features and penetrative total strain across the Clover Hollow anticline. Strain by differing mechanisms in various lithologies was isolated and measured in an attempt to determine the effects of each mechanism. Strain markers within the study area were the following:

(1) Reductions spots in calcareous mudrock (Moccasin Formation). 25–50 shape ratios were measured for XZ, XY and YZ principal strain ellipsoid sections, respectively (principal axes $X > Y > Z$). Irregular pretectonic shapes were removed from the strain determination (see Tobisch *et al.* 1976, fig. 10).

(2) Mudcracks on bedding surfaces of thin limestone layers (Moccasin Formation). Strain determination involved vector summation of mudcrack polygon segment orientations. The method assumed the original undeformed polygonal pattern approximated to a distribution of random lines. The strain ratios (R_s) were

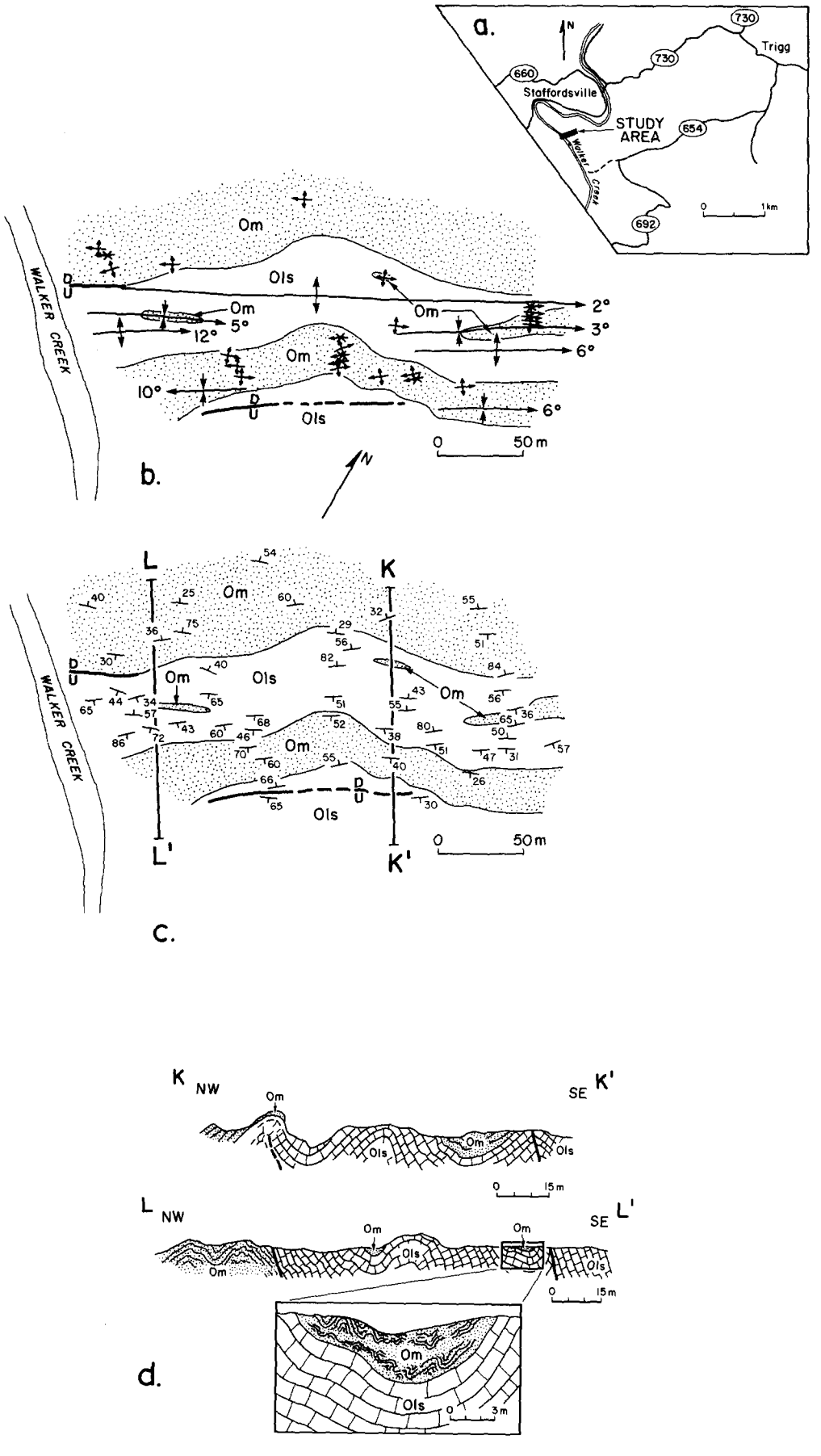

Fig. 11. Complex folding in upper Middle Ordovician limestone (Ols) and Moccasin Formation (Om). (a) Location map of area (see also Fig. 1b). (b) Geologic map with lithologic contacts and fold axes. (c) Geologic map with dip and strike of bedding. (d) Structure sections L–L′ and K–K′. Locations are shown in (c). Enlarged portions shows tight polyclinal folds in the basal Moccasin limestone. Minor symmetry variations indicate hinge migration has occurred.

Table 1. Cleavage intensity classification used for limestone and argillaceous limestone

	WEAK	MODERATE	STRONG
Thickness	< 0.1–3 mm	< 1–4 mm	2–6 mm
Spacing	3–10 cm	1–3 cm	< 0.5–2 cm
Morphology	stylolitic to undulose; highly anastomosing; sharp; tapered and branching.	undulose, some planar; anastomosing to planar networks; tapered, branching; dendritic; sharp to compound.	planar, some undulose; planar network to anastomosing; sharp to compound; tapered to dendritic.

Morphologic terminology is combined from Alvarez *et al.* (1978), Geiser & Sansone (1981), Powell (1979).

derived from the resultant vector magnitude using the method of Sanderson (1977, fig. 2).

(3) Thin limestone layers with apparent offsets along spaced cleavage (Moccasin Formation) (see Gray 1981b, fig. 1). Longitudinal strain (shortening) due to pressure solution was calculated by comparing present length with reconstructed length (both measured normal to cleavage) of layers oblique to cleavage. They were constructed by pulling apart offset segments to form a continuous layer (see Alvarez *et al.* 1975, fig. 5). Measurements were not undertaken where shear veins were present along the spaced cleavages.

(4) Folded limestone and sandstone layers (Moccasin Formation) and folded limestone (Middle Ordovician limestone). Longitudinal strains (shortening) due to buckling were determined by comparing folded length with the arc length of the layers. Two dimensional 'flattening' strain ratios (R_f) associated with sandstone and limestone fold-shape modification, were determined from orthogonal-thickness measurements in profile sections using a modified t'_α method (see Gray & Durney 1979). R_f values for poorly exposed mesoscopic folds, where interlimb angles could be measured, were obtained from graphed relationships between fold tightness and flattening strains (see Gray 1981a, fig. 9).

Strain determinations for the Middle Ordovician limestones, basal Moccasin Formation and mudrock litho-tectonic units are given in Table 3. The analysis location, strain marker, lithology and inferred deformation mode associated with the strain are given. Total longitudinal natural strain (ε_T) in the Z principal direction, excluding shortening due to contraction faults, has been calculated for each area. Although a non-coaxial history is suggested by relations between cleavage, folds and faults (see next section) actual rotations have been minor (probably less than 10° for YZ sections) and can-

Table 2. Cleavage style across the Clover Hollow anticline

Location	Lithology	Type	Intensity	S_1 Thickness	S_1 Spacing	$S_0 \hat{} S_1$ (degrees)
NW Limb	Ols L	stylolitic to undulose, moderate to highly anastomosing, branching terminations.	weak	< 1–2 mm	1–7 cm	50–90°
	Al	hackly, irregular, branching, undulose, anastomosing to linear, smooth to rough spaced disjunctive.	weak	< 0.1–0.2 mm	< 0.1–3 mm	40–80°
Nose	Ols L	undulose, branching, anastomosing to linear.	moderate to strong	< 1–3 mm	1–3 cm	80–90°
	Cm	linear to slightly anastomosing, planar networks, strong domainal microfabric.	moderate to strong	(< 0.1–0.2 mm)	(< 0.2 mm)	50–90°
SE Limb	Ols L	stylolitic to undulose, branching, anastomosing to linear, compound boundaries.	weak to strong	< 0.1–5 mm	< 1–5 cm	25–90°
	Cm	undulose, linear, planar networks, strong domainal microfabric.	strong	< 0.1–1.5 mm	< 0.1–5 mm	10–90°

Lithology: Ols, Middle Ordovician limestones; Al, argillaceous limestone; L, limestone layer (Moccasin Formation) and Cm, Calcareous mudrock.

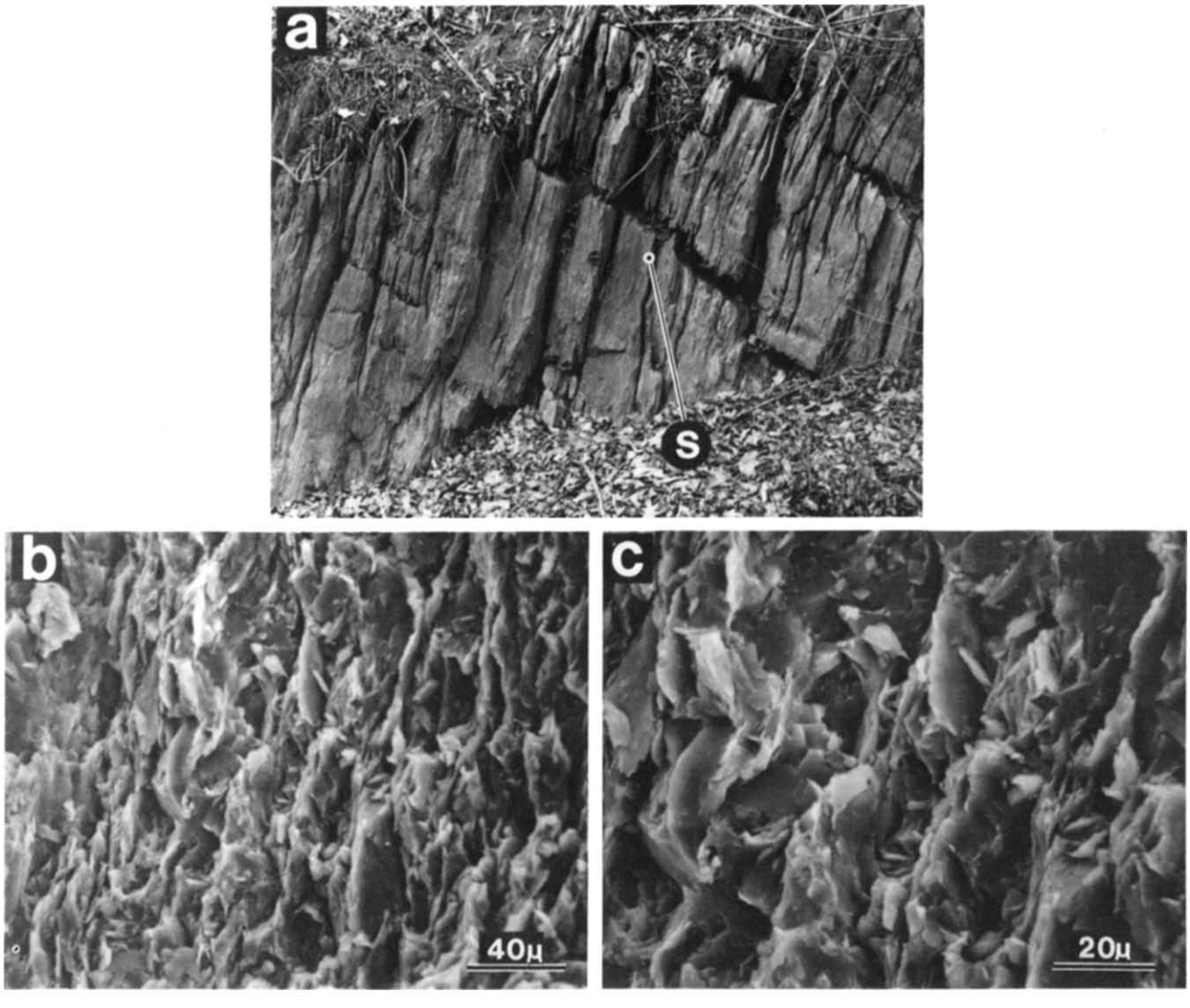

Fig. 12. Cleavages in calcareous mudrock. (a) Outcrop photograph showing the wider spaced, spaced disjunctive cleavage. (b) and (c) SEM micrographs of the domainal microfabric between the spaced cleavage at positon s in (a).

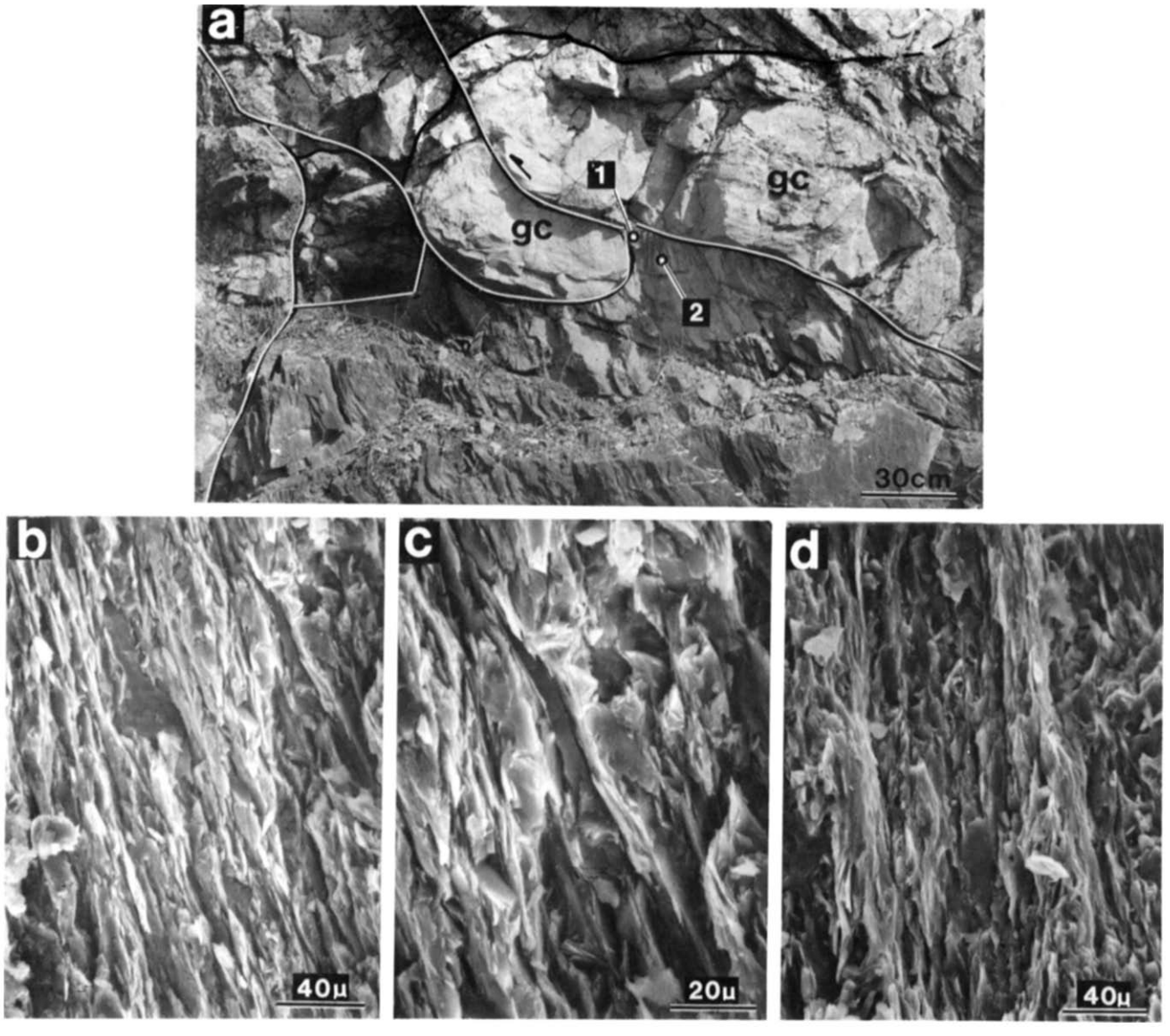

Fig. 14. Modified cleavage microfabric in mudrock adjacent to a third-order contraction fault. Road outcrop on county route 625 near Goodwins Ferry (see Fig. 10a). (a) Imbricate segments of a granule conglomerate layer (gc) are repeated due to contraction faulting. Calcareous mudrock below the fault now occupies irregularities created by the faulting (see position 1). (b) and (c). SEM micrographs of modified cleavage microfabric in the mudrock at 1. (d) SEM micrograph showing a less modified fabric at 2. The microfabric here shows the two fabric components typical of mudrock cleavage microfabrics (see Gray, 1981b).

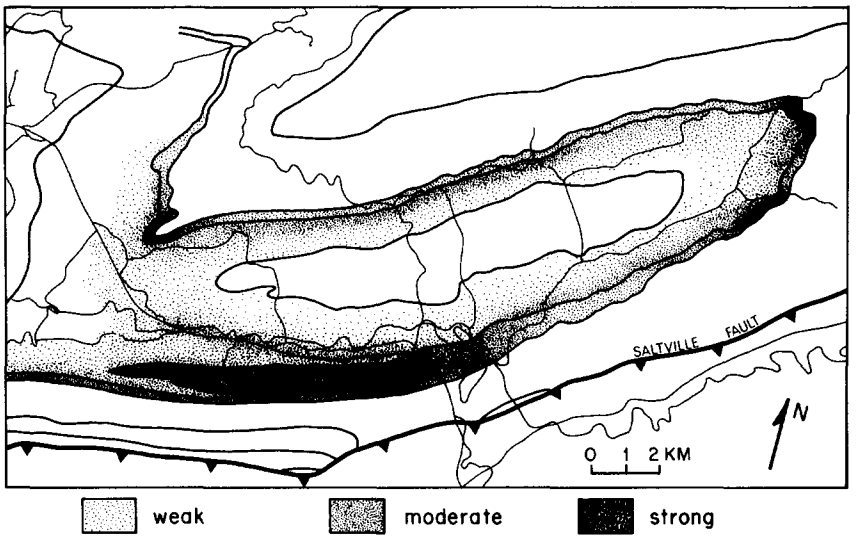

Fig. 13. Cleavage intensity map for the Middle Ordovician limestones and Moccasin Formation of the Clover Hollow anticline. Intensity subdivisions are based on cleavage domain thickness and spacing (see text).

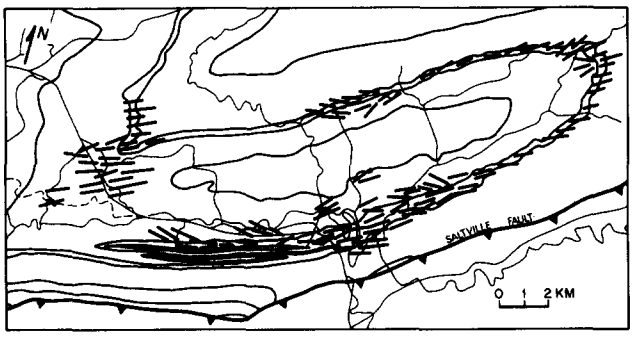

Fig. 15. Regional cleavage orientation based on strike patterns of cleavage planes in Middle Ordovician limestones and Moccasin Formation.

not be precisely determined. For simplicity, therefore, ε_T values were calculated using a coaxial superposition of strains. These therefore only give a first-order approximation of shortening. Furthermore the values may overestimate the total strain by an unknown amount, due to potential overlap of strains from different deformation modes recorded by some markers. This problem will now be discussed.

Reduction spots record three dimensional strain associated with development of a domainal microfabric in the mudrock (see Gray 1981b, fig. 3). They are truncated and offset by the spaced disjunctive cleavage which developed primarily after fold limb dips attained 30° (Gray, 1981a). This strain is considered to represent layer-parallel shortening prior to significant folding. Strain determined from mudcracks is also considered to reflect layer-parallel shortening. Effects of subsequent deformation such as pressure-solution, buckling and fold flattening could potentially modify reduction spot and mudcrack shapes. However, in both cases we maintain that subsequent effects are minimal. Although spaced, stylolitic cleavage sometimes truncates the mudcracks, these do not change the angular relations between adjacent polygon segments. Since Sanderson's method is based on angular relations of the segments the derived mudcrack strain should not record any effects due to pressure-solution. Similarly, reduction spots truncated by the spaced cleavage were not included in the strain analysis. Since the pressure-solution component is specified as that related to development of the spaced disjunctive cleavage (see above) the reduction spot strain cannot be affected by pressure-solution. Effects due to superposition of fold flattening strains are also considered minimal. Mudrocks analysed were in homoclinally dipping strata away from minor fold hinges. These were not affected by the fold-flattening strain increments since this is clearly restricted to fold hinge regions, and varies from fold to fold (see Gray 1981a, fig. 9b). The reduction spots measured were in the thick, relatively homogeneous, sections of mudrock (see Fig. 5) which showed limited effects of folding (e.g. Dieterich 1969, fig. 1c) and consequently little flattening modification. Effects of pressure-solution during fold flattening can also be separated by fold reconstruction after the method of Plessman (1964, fig. 7). Fold-flattening strain analysis was only undertaken on reconstructed folds, such that there was no shape-modification component due to the presence of the spaced cleavage. One problem however, relates to length changes of layers caused by fold-shape modification during fold flattening. Since the buckling strain is determined by comparing arc length with folded length, length changes caused by homogeneous fold-flattening strain could result in a slight overestimate (< 1–2%) of the total strain when buckling and flattening strains are added. We stress once again that ε_T values are first-order approximations of horizontal shortening, but are probably within $\pm 5\%$ of the actual values.

Determination of the longitudinal natural strain (ε_T) in the Z direction for respective lithologies will now be

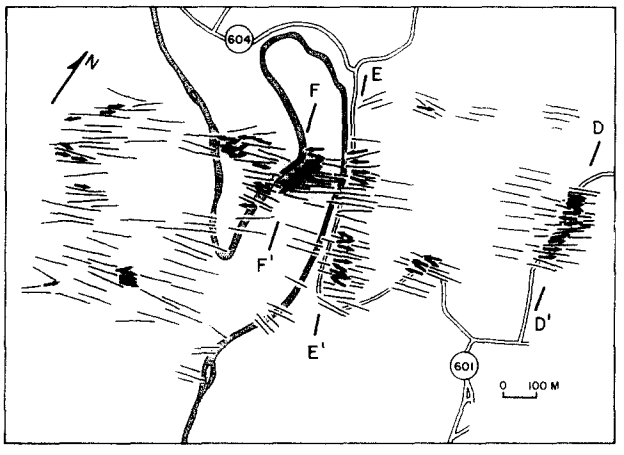

Fig. 16. Patterns of cleavage traces (thin lines) and fold axes (arrows) in an area of intense folding associated with third-order contraction faulting (Group 1 folds). Positions of structure sections D–D', E–E' and F–F' are shown (Figs. 6 and 8).

discussed. Since different deformation mechanisms have dominated in various lithologies, each lithology requires separate treatment. Competent layers, like the Middle Ordovician limestones and basal Moccasin member have undergone layer-parallel shortening, buckling, flattening and pressure-solution (Gray 1981a, b). The principal natural shortening strain (ε_T) is:

$$\varepsilon_T = \varepsilon_{lps} + \varepsilon_b + \varepsilon_f + \varepsilon_{ps},$$

where ε_{lps} = layer-parallel shortening strain, ε_b = buckling strain, ε_f = fold-flattening strain and ε_{ps} = pressure-solution strain. Incompetent Moccasin mudrock experienced layer-parallel shortening and pressure-solution deformation. Other processes did not significantly contribute to total strain. For mudrock sections, total strain (ε_T) is largely given by:

$$\varepsilon_T = \varepsilon_{lps} + \varepsilon_{ps}.$$

Table 3. Strain partitioning data from Clover Hollow anticline. Locations are shown in Fig. 6. Om, Moccasin Formation; Ols, Ordovician limestones.

LOCALE	MARKER	LITHOLOGY	STRAIN PARAMETER	ϵ_T	DEFORMATION MODE
1	reduction spots	mudrock	X:Y:Z = 1.78:1:0.55	-0.59	Layer-parallel shortening
	folded limestone layer	limestone (Om)	Z = 0.63	-0.46	Buckling
	folded limestone layer	limestone (Om)	X/Z = 1.4	-0.16	'Flattening'
	offset limestone interbeds in mudrock	mudrock	Z = 0.54	-0.62	Pressure-solution
2	reduction spots	mudrock	X:Y:Z = 2.06:1:0.52	-0.65	Layer-parallel shortening
	reduction spots	limestone (Om)	X:Y:Z = 1.26:1:0.79	-0.24	
	mudcracks	limestone (Om)	Y/Z = 0.63	-0.47	
	folded limestone layer	limestone (Om)	Z = 0.82	-0.20	Buckling
	folded sandstone layer	sandstone (Om)	X/Y = 1.4	-0.16	'Flattening'
	folded limestone layer	limestone (Om)	X/Y = 1.6	-0.23	
	offset limestone interbeds in mudrock	mudrock	Z = 0.58	-0.54	Pressure-solution
3	reduction spots	mudrock	X:Y:Z = 2.64:1:0.47	-0.76	Layer-parallel shortening
	mudcracks	mudrock	Y/Z = 0.63	-0.47	
	folded limestone layer	limestone (Om)	Z = 0.65	-0.43	Buckling
	folded limestone layer	limestone (Ols)	Z = 0.76	-0.27	
	folded limestone layer	limestone (Om)	X/Z = 2.1	-0.31	'Flattening'
	folded limestone layer	limestone (Ols)	X/Z = 1.65	-0.22	
	offset limestone interbeds in mudrock	mudrock	Z = 0.55	-0.60	Pressure-solution
4	reduction spots	limestone (Om)	X:Y:Z = 1.61:1:0.63	-0.46	Layer-parallel shortening
	mudcracks	limestone (Om)	Y/Z = 0.53	-0.63	
	folded limestone layer	limestone (Om)	Z = 0.90	-0.11	Buckling
	folded limestone layer	limestone (Ols)	Z = 0.80	-0.22	
	folded limestone layer	limestone (Om)	X/Z = 0.30	negl.	'Flattening'
	folded limestone layer	limestone (Ols)	X/Z = 1.2	-0.09	
	offset limestone interbeds in mudrock	mudrock	Z = 0.74	-0.30	Pressure-solution

The argillaceous limestone of the Moccasin Formation has a significant ratio of fold-amplification to layer-parallel-shortening. Total strain for this unit, is

$$\varepsilon_T = \varepsilon_{lps} + \varepsilon_b + \varepsilon_{ps}.$$

Sufficient data for these calculations were obtained from three locations on the southeast limb of the structure and one location on the northwest limb (Fig. 6). A summary of total natural strain (ε_T) calculated for the limestones and Moccasin Formation across the regional structure includes the following.

Southeast Limb.	
Location 1	ε_T(limestones) = −1.21 (70% shortening)
	(mudrock) = −1.19 (70% shortening)
Location 2	ε_T(limestones) = −1.24 (71% shortening)
	(mudrock) = −1.21 (70% shortening)
Location 3	ε_T(limestones) = −1.56 to −1.81 (79 to 84% shortening)
	ε_T(mudrock) = −1.36 (74% shortening)
Northwest Limb.	
Location 4	ε_T(limestones) = −0.31 (27% shortening)
	(argillaceous limestones) = −0.087 (58% shortening)

The above ε_T values indicate relatively close agreement in magnitudes of total natural longitudinal strain from different lithologies at the various locations. Lateral shortening, measured at the outcrop scale, varies across the regional structure. Strains (ε_T) along the southeast limb were similar in two locations (1 and 2) while strain values closer to the Saltville fault (location 3) appear higher. Strains on the northwest limb of the Clover Hollow anticline are less than those measured on the southeast limb.

The strain data (Table 3) shows considerable variability of calculated strains for deformation modes at different structural positions across the Clover Hollow anticline. Buckle, pressure-solution and fold-flattening strain values are higher on the southeast limb of the regional structure. Strain components due to pressure-solution and flattening are lower or negligible on the northwest limb. Layer-parallel shortening values also show significant variations across the structure. Systematic repetition of the sandstone member of the Moccasin Formation along the southeast limb of the Clover Hollow anticline provides a marker bed for calculation of macroscopic buckling and faulting strain shortening. Measurements of fold arc-lengths after removing fault displacements (and assuming uniform layer thickness) give values of 27–29% shortening due to buckling with 25–35% shortening attributed to displacements along third-order contraction faults.

Axial ratios of strain ellipsoids determined from reduction spots (Table 4) are lower on the northwest limb than the southeast limb of the Clover Hollow anticline (Fig. 17). Within each limb there is least variance in X/Y, intermediate variance in Y/Z and maximum variance in X/Z. Strain data plots within the constriction field near plane strain (Fig. 18); k values (Flinn 1962) range from 0.95 to 4.50, whereas Lodes numbers (Hossack 1968) range from −0.02 to −0.64 (Table 4). Trends on the graphs (Figs. 18, a and b) may define a strain path representing variation in the state and magnitude of total strain during a progressive deformation (see Wood 1974). The path moves from approximate plane strain into the constriction field with increasing strain intensity. Axial ratios are highest close to the Saltville fault with a steady decrease away from the fault trace to the northwest limb. The pattern does not conform to deformations involving compaction (Sanderson 1976, Graham 1978). All ellipse long axes are at high angles to bedding.

IMPLICATIONS OF MESOSCOPIC STRUCTURE AND STRAIN

Interrelations between mesoscopic folds, second- and

Table 4. Reduction spot analysis Nadai graph data

Location*	X/Y	Y/Z	X/Z	γ_0	v	k	$\bar{\varepsilon}_s$
1	2.638	2.139	5.640	1.156	−0.18	1.44	1.000
2	2.296	1.938	4.450	1.074	−0.16	1.38	0.930
3	1.782	1.824	3.251	0.954	+0.03	0.95	0.830
4	1.706	1.610	2.760	0.844	−0.07	1.16	0.766
5	1.606	1.580	2.550	0.849	−0.02	1.04	0.735
6	2.060	1.923	3.962	1.031	−0.07	1.15	0.893
7	1.810	1.180	2.150	0.767	−0.64	4.50	0.664

* Locations given in Fig. 17.

Reduction spot axial ratios were converted to natural strain. Lode's numbers and 'k' values (Hossack 1968).

Equations: $a = \dfrac{\text{major axis}}{\text{intermediate axis}}$, $b = \dfrac{\text{intermediate axis}}{\text{minor axis}}$

$$k = \frac{a-1}{b-1}, \quad v = \frac{1-k}{1+k}$$

$$\gamma_0 = \frac{4}{3}\left[\log\left(\frac{X}{Y}\right)^{1/2} + \log\left(\frac{Y}{Z}\right)^{1/2} + \log\left(\frac{X}{Z}\right)^{1/2}\right]^{1/2}$$

$$\bar{\varepsilon} = (\sqrt{3/2})\gamma_0.$$

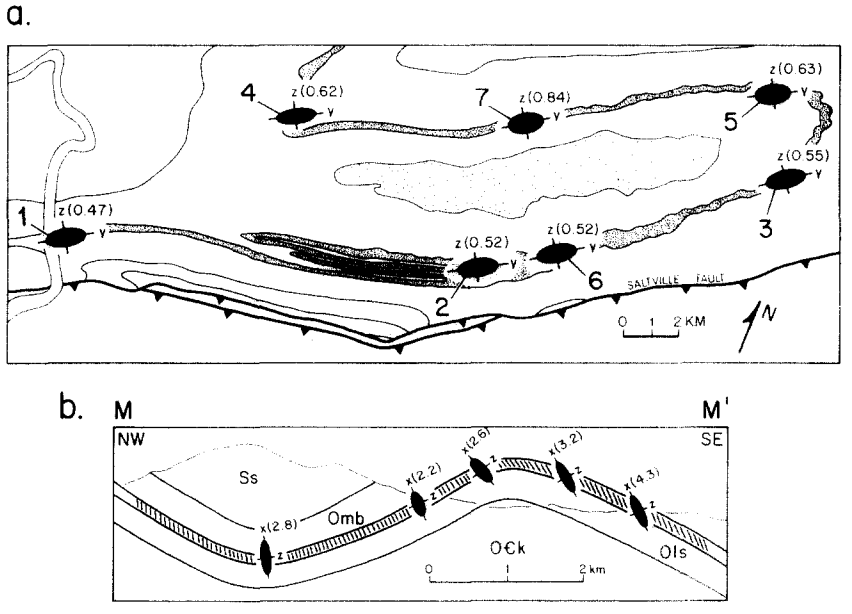

Fig. 17. Area variation in strain determined from reduction spots in calcareous mudrock of the Moccasin Formation. Strain data are from Table 4. (a) ZY principal strain variation map across the Clover Hollow anticline. Actual Z/Y strain values are given in parentheses. (b) Down-plunge projection of map data across the Clover Hollow anticline and Johns Creek syncline. Cleavage traces (thin lines) and X/Z values (in parentheses) are shown. Lithologies as Fig. 6.

third-order contraction faults, and cleavage define a distinct structural style for these Appalachian Valley and Ridge Province rocks. The distribution of structures and intensity of deformation are spatially associated with second- and third-order contraction faults (Figs. 7 and 9). Strain magnitude and horizontal shortening (ε_T) are highest where contraction faults locally dominate the structure (Table 3). Fold tightness and cleavage intensity (Fig. 13) are also maximum in strata within and adjacent these faults.

Faulting and the associated complex structural development is most significant along the southeast limb of the Clover Hollow anticline (Figs. 3 and 9a). Similar relationships do not occur on southeast dipping limbs of other small regional folds within the northwest portion of the Narrows thrust sheet. This suggests that structural complexity is due to proximity to the Saltville fault (Figs. 1, 3 and 7). Second-order faults have high dips but show variations related to the competency of the strata. High fault dips occur in competent units such as the Middle Ordovician limestones, whereas lower dips, often subparallel to bedding, occur in weaker strata such as the Moccasin Formation (Fig. 10a). These relationships and the trajectories of some third-order faults, suggest that contraction faults have a listric form and dips decrease with depth. The presence of Middle Ordovician limestone, basal Moccasin limestone and Martinsburg shale along the hanging wall traces of the second-order faults (Fig. 9c) indicates that detachment has occurred in the upper portion of the Middle Ordovician limestones, at the base of the Moccasin Formation and within the Martinsburg Formation. The faults probably represent splay thrusts subsidiary to the main Saltville thrust (Fig. 2). Zones of third-order faults are laterally continuous with, and transitional into, second-order faults (Fig. 9a). This is a displace-

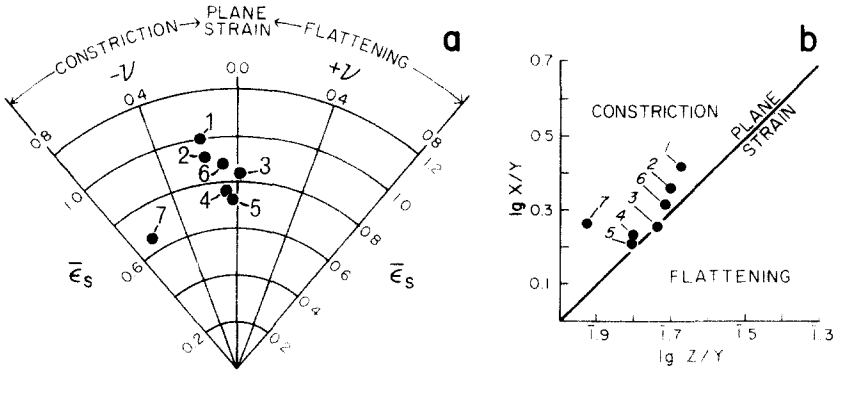

Fig. 18. Reduction spot strain plots (a) Hsu diagram (Nadai graph) with strain magnitude ($\bar{\varepsilon}_s$) and Lode's ratio (V) on a polar graph. (b) Logarithmic Flinn diagram. Points represent means of 25–50 measurements at seven localities (see Fig. 17a and Table 4).

ment transfer (Dahlstrom 1970) phenomenon where shortening accommodated along one or two larger faults is transferred into a zone of numerous smaller mesoscopic (third-order) faults. Third-order contraction faults represent strain accommodation where local folding and cleavage development could not keep pace with deformation. 'Locking' of folds (Ramsay 1974, Cobbold, 1976) caused development of limb thrusts (Ramsay op. cit., fig. 11) where the fault surfaces lie along or close to bedding on southeast dipping limbs but truncate layering on northwest dipping limbs. These faults dominate sections of the Moccasin Formation and produce a characteristic structural style (Figs. 8a & c). The geometry and association of faults could have arisen in the following ways:

(1) Divergent and upward-fanning listric faults with interconnected splays solely in the Moccasin Formation. Thrust initiation and termination loci would be randomly distributed in the unit. Faulting in other units would be unrelated to structural development in the Moccasin Formation.

(2) Imbricate fans of listric faults which initiate from a common décollement in the underlying limestone lithologies. Other fault imbricates would be associated with detachments in the Eggleston or Martinsburg formations.

(3) A duplex in which a series of imbricate thrusts are bounded by roof and floor thrusts (cf. Elliott and Johnson 1980). Potential floor thrusts are the underlying décollements in the uppermost Middle Ordovician limestones, or at the Moccasin–Middle Ordovician limestone contact. Roof thrusts possibly exist in the overlying Eggleston or Martinsburg formations.

Field relations shown in the structure sections indicate that cases 1 and 2 are both probably responsible for tectonic thickening of the Moccasin Formation. Case 1 applies to areas where the Moccasin–Middle Ordovician limestone contact is structurally conformable (Fig. 9c, section I–I′ and Fig. 11d, section K–K′ and C–C′). Case 2 occurs in association with detachment at the limestone–mudrock contact (Figs. 7b, 9b and 11c). The system of contraction faults along the southeast limb of the anticline (Fig. 9a) has a duplex-like form (case 3), but the essentially two-dimensional nature of the outcrop does not allow for proof of this.

Mesoscopic fold generation is closely associated with second-order contraction faults. Although some open folds observed on the NW limb of the Clover Hollow anticline must have been initiated as parasitic structures, areas of intense folding only occur near these faults. Tight to close folds (Group 1 folds) occur adjacent to terminal zones of the large, second order contraction faults (Figs. 8a–c); they are truncated by third-order contraction faults and have undergone tightening, hinge migration (see Gray 1981a, p. 269) and cleavage intensification during faulting. Other areas of intense folding (Group 2 folds) occur above detachment zones associated with second-order contraction faults at the Moccasin–Middle Ordovician limestone contact (Fig. 7b). These polyclinal folds largely occur in the thin-bedded basal limestone of the Moccasin Formation. They are disharmonic with the overlying and underlying structures and must have been initiated as perturbations along the developing dislocation zone for the second-order faults.

Field relations (Figs. 7a, 8c and 9c) suggest that in general, minor folding and cleavage development preceded faulting. It is proposed that zones of high strain-rate developed with folding and intense cleavage, and eventually gave way to faulting. This is typified by the transition of second-order contraction faults (Fig. 9a) into regions where minor folds are truncated by third-order contraction faults (Fig. 8a). After third-order faults developed there was little internal strain by buckling and cleavage development, although in some cases cleavage fabrics were modified adjacent to the faults (Fig. 14). Cleavage-fold relations of the minor folds on the southeast limb of the Clover Hollow anticline (e.g. Figs. 8a–c) require pre-folding initiation of cleavage perpendicular to bedding (Gray 1981a). Transection of folds by the cleavage (Fig. 15) is considered to be due to a non-coaxial deformation involving sequential and protracted development of cleavage, folds and faulting. The non-coincidence between orientations of cleavage, mesoscopic fold trends and third-order faults (Fig. 5, compare, d. e, f, g, i and j) may imply progressive deformation involving minor rotation of stress and/or strain axes. Such rotations are probably a consequence of thrust-sheet emplacement.

Variations in the orientation and magnitude of reduction-spot strains across the Clover Hollow anticline (Fig. 18a) provide constraints for discriminating whether the anticline developed by upwarping above a subsurface ramp (Rich 1934, Harris & Milici 1977) or due to regional buckling. Experimental analogues of folds produced by a step-like climb of detachment thrusts along tectonic ramps (House & Gray 1982, fig. 11) show that maximum strain intensity would occur on the northwest limbs of such fold structures. This is not in agreement with the observed strain pattern. This, together with the open, symmetrical nature of these smaller regional folds (Figs. 2 and 17b) suggest they are buckle folds associated with lateral shortening of the thrust-sheet above a subsurface décollement. Subsequent modification of the initial structure to produce greater intensity of folding and cleavage, and high strains, on the southeast limb, is considered due to second-order faulting related to emplacement of the Saltville thrust-sheet.

Oblique fanning of cleavage in the Moccasin Formation across the anticline (Fig. 17b) is either due to hinge migration during this subsequent modification (Borradaile 1979) or to initial inclination of the layering to the maximum principal compressive stress (Treagus 1981). However, lack of coincidence between the present hinge (defined by the point of maximum hinge curvature) and the former hinge (where bedding and cleavage are at 90°) suggests that regional fold-hinge migration was responsible for oblique fanning of cleavage and strain trajectories.

CONCLUSIONS

Local and regional strain patterns across the Clover Hollow Anticline show a distribution related to the presence of contraction faults and to regional fold-hinge migration. Buckling rather than upwarping due to the presence of a subsurface ramp is considered responsible for the small regional folds within the Narrows thrust-sheet. Faults dominate the structure at all scales. Fold tightness, cleavage intensity, strain magnitude and computed total natural strain (ε_T) in the Z principal direction are maximum where second- and third-order contraction faults are present. Cleavage orientation and microfabrics, particularly in mudrock, are modified adjacent to these faults. Two groups of mesoscopic folds are associated with the contraction faults. Tight, polyclinal to chevron folds (Group 2 folds) developed in detachment zones along stratigraphic contacts in response to second-order faults. Other zones of intense folding (Group 1 folds), associated with third-order contraction faults, are considered to be displacement transfer phenomena at the lateral terminations of second-order contraction faults in series.

Cleavage morphology, intensity and orientation vary locally and regionally. Map patterns and stereogram analysis of cleavage-fold relations reveal regional fold transection. Competent limestones exhibit greater Δ transection values than Moccasin calcareous mudrock. Strong cleavage intensity and greater finite strains occur on the southeast limb of the regional fold. Calculations of ε_T across the region, derived from reduction spots, mudcracks, fold-flattening, pressure-solution offsets, and buckle and fault shortening (but excluding shortening due to contraction faulting) revealed higher strains ($\varepsilon_T \sim -1.21$) for the southeast limb than for the northwest limb ($\varepsilon_T \sim -0.87$) of the regional fold. These relationships, not shown by smaller regional folds to the northeast, suggest that structural and deformation fabrics within this portion of the Narrows thrust-sheet were affected by deformation associated with emplacement of the Saltville thrust-sheet to the southeast (Fig. 2). This may have implications for the relative timing of thrust-sheet emplacement.

Association of second- and third-order contraction faults with intense cleavage and mesoscopic folding, are quite distinct in the Narrows thrust-sheet. This, combined with overprinting criteria for fabric and mesoscopic structural elements, suggests that minor faults which accompany internal thrust-sheet distortion under anchimetamorphic conditions develop in regions of high strain-rate where intense cleavage and tight to close mesoscopic folding predominate.

Acknowledgements—The work was completed by R.I.S. as part of the requirements for an M.Sc. degree at Virginia Polytechnic Institute and State University. Academic year support was provided by a Departmental Graduate Teaching Assistantship. Field support was by a Grant-in-Aid from Sigma Xi (The Scientific Research Society of North America) and a research grant from the Geological Society of America, all awarded to R.I.S. Summer support was from National Science Foundation Grant No. EAR. 79-19703 awarded to D.R.G.

We gratefully acknowledge former students at V.P.I. & S.U. whose M.Sc. work provided the basic field maps which made detailed structural analysis possible. These include T. Y. Frieders, J. A. Gambill, C. R. Hobbs, A. T. Ovenshire and C. R. Moon. We also thank W. D. Lowry and L. Glover, III for their helpful comments on an early version of the manuscript and David Elliott for helpful discussion about down-plunge projection techniques. Assistance for paper preparation was given by V.P.I. & S. U.; thanks are extended to Martin Eiss and Sharon Chiang for drafting, Donna Williams for typing and Cynthia Zauner for photography.

REFERENCES

Alvarez, W., Engelder, T. & Geiser, P. 1978. Classification of solution cleavage in pelagic limestones. *Geology* **6,** 263–266.

Borradaile, G. J. 1978. Transected folds: a study illustrated with examples from Canada and Scotland. *Bull. geol. Soc. Am.* **89,** 481–493.

Borradaile, G. J. 1979. Strain study of the Caledonides in the Islay region, S. W. Scotland: implications for strain histories and deformation mechanisms in greenschists. *J. geol. Soc. Lond.* **136,** 77–88.

Cloos, E, 1947. Oolite deformation in the South Mountain fold, Maryland. *Bull. geol. Soc. Am.* **58,** 843–918.

Cobbold, P. R. 1976. Fold shapes as functions of progressive strain. *Phil. Trans. R. Soc. Lond.* **A283,** 129–138.

Dahlstrom, C. D. A. 1970. Structural geology in the eastern margin of the Canadian Rocky Mountains. *Bull. Can. Petrol. Geol.* **18,** 322–406.

Dieterich, J. H. 1969. Origin of cleavage in folded rocks. *Am. J. Sci.* **267,** 155–165.

Elliott, D. & Johnson, M. R. W. 1980. Structural evolution in the northern part of the Moine thrust belt, NW Scotland. *Trans. R. Soc. Edinb.*, Earth *Sci.* **71,** 69–96.

Epstein, A. G., Epstein, J. B. & Harris, L. D. 1976. Conodont color alteration — an index to organic metamorphism. *Prof. Pap. U. S. geol. Surv.* **995,** 1–27.

Flinn, D. 1962. On folding during three-dimensional progressive deformation. *J. geol. Soc. Lond.* **118,** 385–433.

Geiser, P. A. & Sansone, S. 1981. Joints, microfractures, and the formation of solution cleavage in limestone. *Geology*, **9,** 280–285.

Graham, R. H. 1978. Quantitative deformation studies in the Permian rocks of Alpes-Maritimes. *Proc. Symposium in honour of Prof. J. Goguel.* BR.G.M. Paris, 212–238.

Gray, D. R. 1981a. Cleavage-fold relationships and their implications for transected folds: an example from southwest Virginia, U.S.A. *J. Struct. Geol.* **3,** 265–277.

Gray, D. R. 1981b. Compound tectonic fabrics in singly-folded rocks from southwest Virginia, U.S.A. *Tectonophysics.* **78,** 229–248.

Gray, D. R., and Durney, D. W., 1979. Investigations on the mechanical significance of crenulation cleavage. *Tectonophysics* **58,** 35–79.

Gwinn, W. E., 1964. Thin-skinned tectonics in the plateau and north western Valley and Ridge provinces of the Central Appalachians. *Bull. geol. Soc. Am.* **75,** p. 863–900.

Harris, L. D. & Milici, P. C. 1977. Characteristics of thin-skinned style of deformation in the Southern Appalachians, and potential hydrocarbon traps. *Prof. Paper U. S. geol. Surv.* **1018,** 1–40.

Hobbs, B. E. 1971. The analysis of strain in folded layers. *Tectonophysics* **11,** 329–375.

Hossack, J. R. 1968. Pebble deformation and thrusting in the Bygdin area (Southern Norway). *Tectonophysics* **5,** 315–339.

House, W. M. & Gray, D. R. 1982. Displacement transfer at thrust terminations in southern Appalachians — Saltville thrust as an example. *Bull Am. Ass. Petrol. Geol.* (July issue).

Milici, R. C. 1970. The Allegheny structural front in Tennessee and its regional tectonic implications. *Am. J. Sci.* **268,** 127–141.

Milnes, A. G. 1971. A model for analyzing the strain history of folded competent layers in deeper parts of orogenic belts. *Eclog. Geol. Helv.* **64,** 335–342.

Mitra, S. 1978. Microscopic deformation mechanisms and flow laws in quartzites within the South Mountain anticline. *J. Geol.* **86,** 129–152.

Plessmann, W. 1964. Gesteinlösung, ein Hauptfaktor beim Schieferungsprozess. *Geol. Mitt.* **4,** 69–82.

Powell, McA. 1979. A morphological classification of rock cleavage *Tectonophysics* **58,** 21–34.

Price, R. A. 1967. The tectonic significance of mesoscopic subfabrics in the southern Rocky Mountains of Alberta and British Columbia *Can. J. Earth Sci.* **4,** 39–70

Ramsay, J. G. 1967. *Folding and Fracturing of Rocks.* McGraw Hill, New York.

Ramsay, J. G. 1974. Development of chevron folds. *Bull. geol. Soc. Am.* **85,** 1741–1754.

Ramsay, J. G. 1981. Tectonics of the Helvetic Nappes. In: *Thrust and Nappe Tectonics* (edited by McClay, K. & Price, N.J.) *Spec. Publs geol. Soc. Lond.* **9,** 293–304.

Rich, J. L., 1934. Mechanics of low-angle overthrust faulting as illustrated by Cumberland thrust block, Virginia, Kentucky, and Tennessee. *Bull. Am. Ass. Petrol. Geol.* **18,** 1584–1596.

Sanderson, D. J. 1976. The superposition of compaction and plane strain. *Tectonophysics* **30,** 35–54.

Sanderson, D. J. 1977. The analysis of finite strain using lines with an initial random orientation. *Tectonophysics*, **43,** 199–211.

Tan, B. K., 1976. Oolite deformation in Windgällen, Canton Uri. *Tectonophysics* **31,** 157–174.

Tobisch, O. T. Fiske, R. S. Sacks, S. & Taniguchi, D. 1977. Strain in metamorphosed volcaniclastic rocks and its bearing on the evolution of orogenic belts. *Bull. geol. Soc. Am.* **88,** 23–40.

Treagus, S. H. 1981. A theory of stress and strain variations in viscous layers, and its geological implications. *Tectonophysics* **72,** 75–103.

Wood, D. S. 1974. Current views of the development of slaty cleavage. *A. Rev. Earth Planet. Sci.* **2,** 369–401.